

Infrared 3D Observations of Nearby Active Galaxies

R. Maiolino¹, N. Thatte², A. Alonso-Herrero³, D. Lutz², A. Marconi¹

¹*Osservatorio Astrofisico di Arcetri, Firenze, Italy*

²*Max-Planck-Institut für Extraterrestrische Physik, Garching, Germany*

³*Steward Observatory, Tucson, Arizona*

Abstract. We present multi-wavelength imaging observations of three nearby and famous active galaxies obtained with NICMOS, ISOCAM and the MPE near-IR integral field spectrometer. The data reveal a variety of features and properties that are missed in optical studies and in traditional IR monodimensional spectroscopy.

1. Introduction

Infrared observation of active galaxies (starbursts and AGNs) have greatly improved our understanding of these systems, not only because they are usually heavily obscured at optical wavelengths, but also because the infrared bands offer a wealth of indicators that often do not have an equivalent in the optical range. Over the past few years, new IR instruments and observing facilities have provided two-dimensional spectroscopic information of these systems through integral field spectroscopy and narrow band imaging. New integral field spectra obtained with the MPE 3D near-IR spectrometer, NICMOS-HST narrow and broad band images and ISOCAM-CVF spectra of three nearby and famous active galaxies allowed a detailed investigation of their nuclear region revealing new features and properties, and showing that optical observations and traditional IR spectroscopy only provide a limited view of this class of objects. Here we summarize some of the results based on these data.

2. NGC1068

This famous galaxy is regarded as the archetype of Seyfert 2 galaxies. The [OIII]5007Å map shows an ionization cone to the North-East of the nucleus, and a much fainter counter-cone to the South-West. The morphology and the dynamics of the Narrow Line Region (NLR) appear affected by the radio jets (eg. Axon et al. 1998). The radio jets also feed two large scale radio lobes.

We observed the nuclear region of NGC1068 with 3D, the MPE near-IR integral field spectrometer (Weitzel et al. 1996), assisted by ROGUE, a first order adaptive optics system (Thatte et al. 1995), at the William Herschel Telescope (WHT) and at the Anglo Australian Telescope (AAT).

Various IR lines and powerful hot dust emission were detected (Thatte et al. 1997). Here we focus on the properties of the [SiVI]1.96μm high excitation

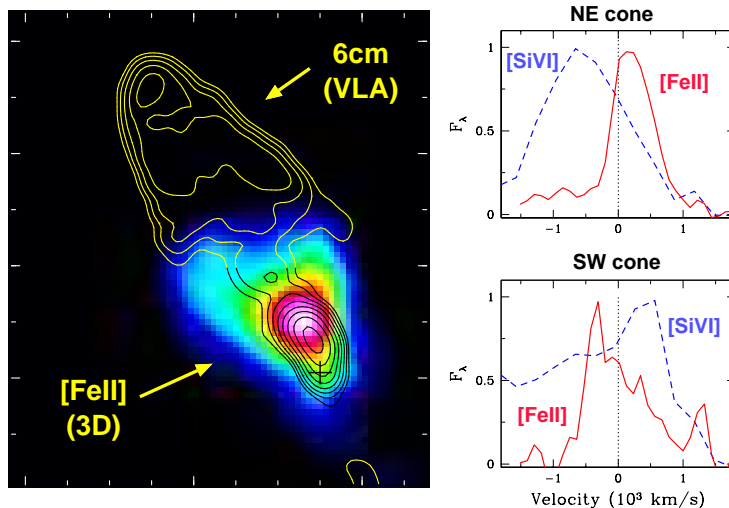


Figure 1. NGC1068. Left: integrated [FeII]1.64 μ m emission obtained with the MPE-3D integral field spectrometer overlaid on the 6cm VLA map of the NE lobe. Right: [FeII]1.64 μ m and [SiVI]1.97 μ m line profiles in the two ionization cones.

coronal line and the [FeII]1.64 μ m line that instead traces the low ionization region. Both lines are detected in the NE ionization cone and, at a lower level, in the SW cone. Overall, the morphology of their integrated emission is similar to the [OIII]-HST map, though at a lower resolution. In Fig. 1 we show the [FeII] map, which has the characteristic cone-like morphology. Given that both these lines are observed in the ionization cones it is tempting to assume that they are emitted by the same population of ionized clouds. However, the kinematics of the gas as traced by the two lines points to a more complex scenario. In Fig. 1 we show the profile of the [FeII] and [SiVI] lines, with respect to the host galaxy systemic velocity. In the NE cone [SiVI] is blueshifted while [FeII] is redshifted and the shift between the two lines is several 100 km/s. In the SW cone the situation is exactly reversed. The large velocity difference between the two lines indicates that they come from different populations of ionized clouds.

We think that the radio lobes affect the kinematics and the ionization structure of the large scale NLR, similar to that observed on smaller scale clouds near the radio jet (Axon et al. 1998). Fig. 2 schematically illustrates our model. In the NE radio lobe (right-hand side in Fig. 2) the upper part of the expanding bow shock accelerates the gas in our direction, hence its emission is blueshifted. This gas is mostly out of the galactic gas disk and, therefore, it has low density, hence high ionization parameter that favors the emission of high ionization species such as Si⁺⁶. On the opposite side the bow shock enters the dense gas of the galactic disk, that is therefore redshifted. Here the bow shock rapidly loses its energy, a fraction of which destroys dust grains returning Fe into the gas phase, thus increasing the [FeII] emission. Also, the high density characterizing this region decreases the ionization parameter, while the column of gas and dust in these equatorial regions hardens the ionizing photon flux; both these effects favor the emission of low ionization lines typical of the transition regions, such

as [FeII]. The symmetric model for the SW cone explains the velocities of [FeII] and [SiVI] inverted with respect to the NE cone.

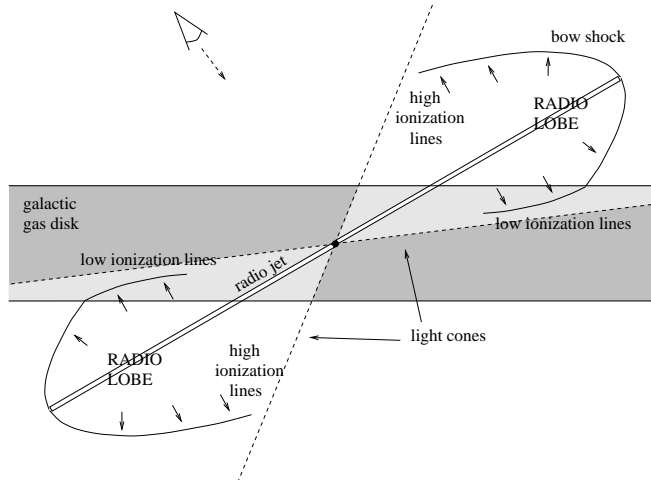


Figure 2. Proposed model for the Narrow Line Region of NGC1068

Although the bow shock returns Fe into the gas phase and produces the observed redshift of the low ionization gas, probably it does not play a major role in exciting the line. Indeed, the [FeII] map has a cone-like morphology, indicating that the nuclear X-ray source is probably responsible for exciting this line.

Finally, the comparison of the radio and [FeII] maps in Fig. 1 further supports our model. The lower end of the radio lobe in Fig. 1 nicely matches the upper end of the [FeII] cone, we think that this dividing line traces the region where the radio lobe enters the galactic gas disk. Therefore, the dense gas south of this line has been Fe-enriched and redshifted, as actually observed. A more detailed discussion of these results is given in Thatte et al. (in prep.).

3. Circinus

At a distance of only 4 Mpc, the Circinus galaxy is the closest *bona fide* Seyfert 2 known. Its proximity makes this galaxy an excellent candidate with which to tackle various issues related to the interaction between active nuclei and their circumnuclear region. Within this context, the mechanism responsible for feeding AGNs on the 10–100 pc scale is a debated issue. Shlosman et al. (1989) and Wada & Habe (1992) proposed that when the mass of the nuclear gas disk is a significant fraction of the dynamical mass (>20%) it becomes gravitationally unstable and forms a gaseous bar that can drive gas into the innermost region to fuel the AGN. Circinus has an extremely gas-rich nuclear region and, therefore, it is an optimal candidate to search for this nuclear gaseous bar.

Broad band and narrow band NICMOS-HST observations of the nuclear region of Circinus were obtained. Fig. 3 shows the H–K color map of the nuclear region (Maiolino et al. 1999). The galaxy major axis is at P.A. $\approx 25^\circ$ and the SE is the near side of the disk. The PSF of the nucleus, dominated by hot

dust emission (Maiolino et al. 1998), has been subtracted in Fig. 3. In the circumnuclear region the H–K map traces the effect of dust reddening. The most interesting feature of this map is the L-shaped dusty feature located to the South-East of the nucleus. We identify the radially extended part of this feature with the gas bar expected to feed the AGN in this system according to models. The deprojected length of the gas bar is about 100 pc. The gaseous nature of this bar is inferred by the lack of a stellar counterpart even in the K band light, where extinction is greatly reduced.

Our interpretation can be checked by looking at the kinematics of the molecular gas. Shocks and torques on the leading side of the bar should remove angular momentum from the gas which should result in a strong velocity gradient and radial inflow motions in this region. We observed the nuclear region of Circinus with 3D+ROGUE at the AAT. Fig. 3 shows the velocity field of the H₂ line at 2.12 μ m. The velocity field of the molecular gas along the leading side of the bar is characterized by a strong velocity gradient and a highly redshifted component (i.e. radially inflowing), just as expected by models. This map not only supports our interpretation of the gas bar, but directly shows radial inflow motions that are probably responsible for the AGN fuelling.

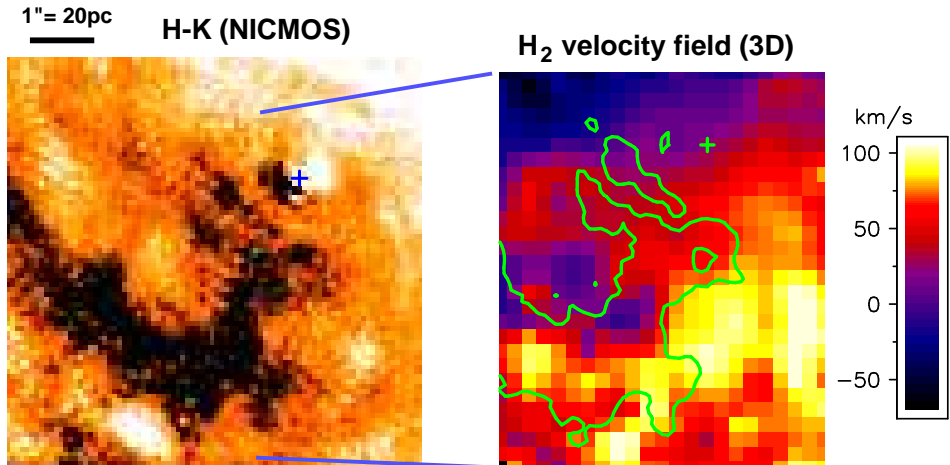


Figure 3. Circinus. Left: H–K NICMOS map; redder colors correspond to darker regions. Right velocity field of the H₂2.12 μ m line obtained with the MPE-3D spectrometer. The cross marks the K-band nucleus.

The large amount of molecular gas driven into the central region also triggers nuclear star formation. Indeed, both Pa α and [FeII] narrow band NICMOS images reveal diffuse circumnuclear emission out of the ionization cone that very likely traces recent star forming activity. A young nuclear stellar population is also inferred from the low mass-to-light ratio as derived from the CO stellar bands at 2.29 μ m observed in the 3D data (Maiolino et al. 1998).

4. NGC4945

Within the context of the starburst-AGN connection, NGC4945 is one of the most spectacular examples of a system where both phenomena coexist. In the

optical and in the IR this edge-on, nearby (3.6 Mpc) galaxy appears as a heavily obscured starburst. However, this galaxy is one of the brightest extragalactic sources at 100 keV, thus revealing the presence of an active nucleus that is heavily absorbed along our line of sight ($N_H \simeq 5 \times 10^{24} \text{cm}^{-2}$).

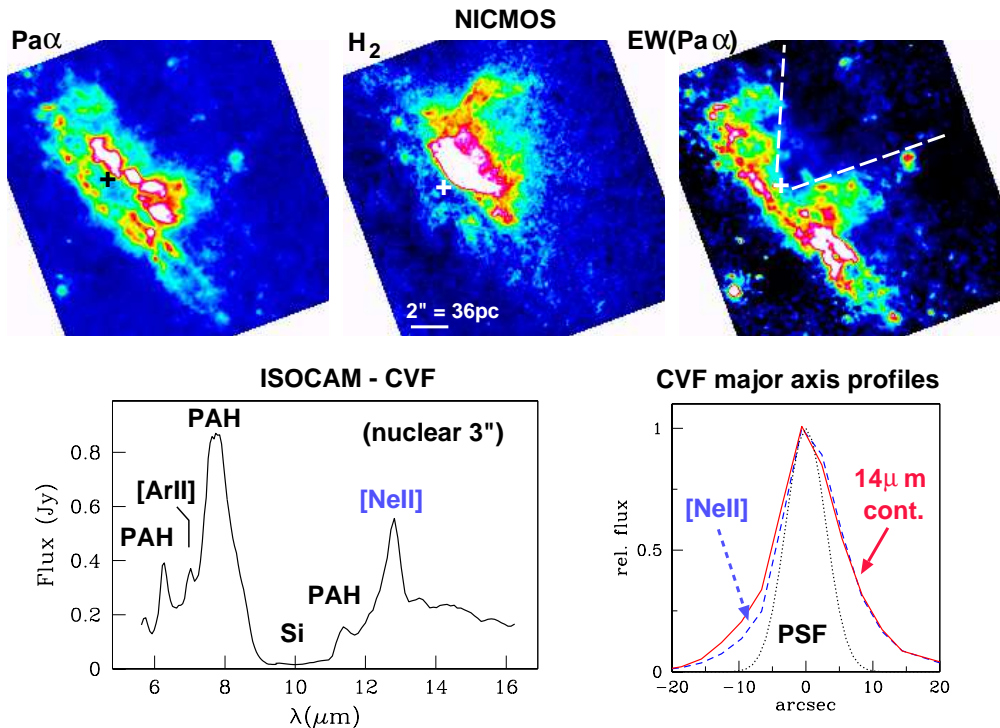


Figure 4. NGC4945. Top: NICMOS images of Pa α (1.87 μm), H₂ (2.12 μm) and Pa α equivalent width; the cross marks the location of the H₂O maser. Bottom: ISOCAM-CVF spectrum of the nuclear region and profiles of the [NeII]12.8 μm line and 14 μm continuum emission along the major axis.

NGC4945 was observed with NICMOS both with broad and narrow band filters (Marconi et al., in prep.). The Pa α image in Fig. 4 reveals a nuclear starburst probably distributed in a ring (about 100 pc in radius) on the galactic plane. Note that this nuclear region is completely obscured at optical wavelengths. The K-band image (not shown) shows no point like source close to the location of the H₂O maser identified by Greenhill et al. (1997). Also, the CO-index map (derived from the NIC2-F237M image) does not provide evidence for a significant dilution of the CO stellar features due to emission of hot dust heated by the AGN. Such emission is instead clearly seen in other similarly obscured AGNs (eg. NGC1068 and Circinus). This indicates that the AGN is obscured along our line of sight even at 2.3 μm . The H₂ 2.12 μm emission line is mostly distributed above the galactic plane (Fig. 4) in a cavity created by the starburst superwind and observed also in the J band images (Moorwood et al. 1996). The lower gas density in the cavity also results in a lower Pa α emission with respect to the continuum, hence lower Pa α equivalent width. Interestingly, the cavity traced by the EW(Pa α) has a cone-like morphology (Fig. 4), similar to the morphology of the NLR in several Sy2 galaxies. However, no UV-ionizing

photons from the AGN reach the gas in the cavity. Indeed, even though plenty of gas is present in the outer parts of the cavity, as traced by the H_2 line and dust filaments, this gas is little ionized and with a spectrum typical of LINERs (possibly excited by the superwind shock). Therefore, the AGN radiation must be absorbed even in the direction of the cone-like cavity. Very likely, the AGN is in a very early stage, still enshrouded in a 4π dusty shell a few pc in size. Given the huge radiation pressure in this region, the dusty shell cannot survive very long. When the dusty shell will break out, then the AGN UV radiation will photoionize the gas within and above the cone-like cavity, transforming the latter into an ordinary ionization cone.

Although the active nucleus is completely obscured even in the K band, we might see its dust emission in the mid-IR, both because the obscuration is further reduced and because warm dust typically emitting at these wavelengths (~ 100 K) is located at larger distances. For this reason ISOCAM-CVF observations of NGC4945 were obtained. Fig. 4 shows the CVF spectrum of the nuclear $3''$. This spectrum shows typical starburst features (strong PAH, [NeII] $12.8\mu\text{m}$ and [ArII] $7\mu\text{m}$ emission), but the saturated silicate absorption feature at $10\mu\text{m}$ indicates that the mid-IR emission comes from a heavily obscured region, with $A_V > 50$ mag. There is some hot dust continuum emission at $14\text{--}16\mu\text{m}$. However, as shown in Fig. 4, this continuum emission is resolved along the galaxy major axis and its distribution is similar to that of [NeII], therefore also the continuum emission is mostly due to the starburst activity. The active nucleus is therefore hidden and undetected even in the mid-IR. Higher angular resolution mid-IR observations are required to check if a weak point-like source might be present on the nucleus.

These results were obtained within a wide collaboration that includes also S. Anders, R. Genzel, D. Macchetto, A. Moorwood, E. Oliva, A. Quillen, M. Rieke, G. Rieke, E. Schreier, E. Sturm, L. Tacconi-Garman and D. Tran.

References

- Axon, D.J., Marconi, A., Capetti, A., Macchetto, F.D., Schreier, E., Robinson, A. 1998 ApJ, 496, L75
- Greenhill, L.J., Moran, J.M., Herrnstein, J.R. 1997 ApJ, 481, L23
- Maiolino, R., Krabbe, A., Thatte, N., Genzel, R. 1998 ApJ, 493, 650
- Maiolino, R., Alonso-Herrero, A., Anders, S., Quillen, A., Rieke, M.J., Rieke, G.H., Tacconi-Garman, L.E. 1999 ApJ, submitt.
- Moorwood, A.F.M., van der Werf, P. P., Kotilainen, J. K., Marconi, A., Oliva, E. 1996 A&A, 308, L1
- Shlosman, I., Frank, J., Begelman, M.C. 1989 Nature, 338, 45
- Thatte, N., Kroker, H., Weitzel, L., Tacconi-Garman, L.E., Tecza, M., Krabbe, A., Genzel, R. 1995 Proceedings of the SPIE, 2475, 228
- Thatte, N., Quirrenbach, A., Genzel, R., Maiolino, R., Tecza, M. 1997 ApJ, 490, 650
- Wada, K., Habe, A. 1992 MNRAS, 258, 82
- Weitzel, L., Krabbe, A., Kroker, H., Thatte, N., Tacconi-Garman, L. E., Cameron, M., and Genzel, R. 1996 A&AS, 119, 531